Evidence of Powerful Substrate Electric Fields in DNA Photolyase: Implications for Thymidine Dimer Repair†

Alexander W. MacFarlane IV and Robert J. Stanley*

Department of Chemistry, Temple University, Philadelphia, Pennsylvania 19122

Received July 9, 2001; Revised Manuscript Received October 8, 2001

ABSTRACT: DNA photolyase is a flavoprotein that repairs cyclobutylpyrimidine dimers by ultrafast photoinduced electron transfer. One unusual feature of this enzyme is the configuration of the FAD cofactor, where the isoalloxazine and adenine rings are nearly in vdW contact. We have measured the steady-state and transient absorption spectra and excited-state decay kinetics of oxidized (FAD-containing, folate-depleted) *Escherichia coli* DNA photolyase with and without dinucleotide and polynucleotide single-stranded thymidine dimer substrates. The steady-state absorption spectrum for the enzyme−polynucleotide substrate complex showed a blue shift, as seen previously by Jorns et al. (*1*). No shift was observed for the dinucleotide substrate, suggesting that there are significant differences in the binding geometry of dinucleotide versus polynucleotide dimer lesions. Evidence was obtained from transient absorption experiments for a long-lived charge-transfer complex involving the isoalloxazine of the FAD cofactor. No evidence of excited-state quenching was measurable upon binding either substrate. To explain these data, we hypothesize the existence of a large substrate electric field in the cavity containing the FAD cofactor. A calculation of the magnitude and direction of this dipolar electric field is consistent with electrochromic band shifts for both $S_0 \rightarrow S_1$ and $S_0 \rightarrow S_2$ transitions. These observations suggest that the substrate dipolar electric field may be a critical component in its electron-transfer-mediated repair by photolyase and that the unique relative orientation of the isoalloxazine and adenine rings may have resulted from the consequences of the dipolar substrate field.

Damage to DNA by ultraviolet light can lead to transcription errors, apoptosis, and cancer (*2*). One of the most frequently observed lesions in DNA is the *cis-syn* cyclobutyl dimerization of adjacent pyrimidines (*3*). Dimerization occurs when the 5,6 double bond from each pyrimidine extends to form a bridge to an adjacent pyrimidine nucleotide, forming a cyclobutyl structure (Scheme 1). These dimers cause a kink in the structure of DNA (*4*) so that it cannot be properly transcribed (*5*) and can block polymerase translocation (*6*). DNA photolyase is a photoactivated flavoprotein that repairs *cis-syn* cyclobutylpyrimidine dimers. It is found in animals, plants, and bacteria (*7*). Flavin adenine dinucleotide (Scheme 2) is present in all photolyases, sometimes as the only chromophore [e.g., *Thermus thermophilus* (*8*)], while other organisms incorporate an additional light harvesting pigment, either 5,10-methylenetetrahydrafolatepolyglutamate (e.g., *E. coli*) or 8-hydroxy-5-deazaflavin (e.g., *Anacystis nidulans*) (*9*).

Scheme 1

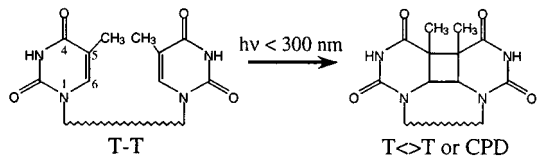

Scheme 2

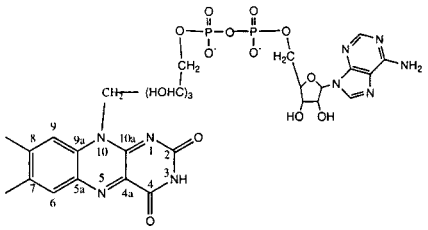

The precise repair mechanism is a matter of conjecture at this time, but there is a consensus on a number of points. In the catalytically active state, the FAD[1] is a fully reduced hydroquinone anion, $FADH^-$. Photolyase repairs the DNA lesion via catalytic electron transfer from $FADH^-$ upon absorption of blue light. The enzyme assumes a one-electron-reduced semiquinone state when the electron has been transferred to the damage site and reverts to $FADH^-$ upon back electron transfer. While the turnover rate for the enzyme is about 3.4 min^{-1} (*10*), both the forward electron transfer to substrate and the reverse electron transfer to regenerate $FADH^-$ are known to be completed within about 2 ns (*11*). Photolyase is enzymatically active without the second

† This research was supported in part by the National Science Foundation (MCB-9982532) and the Petroleum Research Fund (ACS-35353-G4).

* To whom correspondence should be addressed. Phone: (215) 204-2027. Fax: (215) 204-1532. E-mail: rstanley@nimbus.temple.edu.

[1] Abbreviations: FAD, oxidized flavin adenine dinucleotide; CPD, cyclobutylpyrimidine dimer; $FADH^-$ fully reduced anionic FAD; vdW, van der Waals; IPTG, isopropylthiogalactoside; ATP, adenosine triphosphate; EDTA, ethylenediaminetetraacetic acid; PL_{ox}, oxidized DNA photolyase; FMN, flavin mononucleotide; DTT, dithiothreitol.

10.1021/bi0114224 CCC: $20.00
Published on Web 11/13/2001

chromophore (*12*), and its removal simplifies the kinetics of the enzyme by eliminating any energy transfer from the antenna pigment to the flavin cofactor. FAD is an absolute requirement for binding of substrate, though the redox state of the FAD is apparently unimportant for this process, as is the need for light (*13*, *14*).

Although a crystal structure of the *E. coli* enzyme was obtained in 1995 (*15*), there is no structure available for the enzyme−substrate complex. This has led to extensive debate about the enzyme−substrate docking configuration. FAD sits in the bottom of a cavity that leads to the surface of the protein. The opening is flanked by positively charged residues (*15*). Though this is clearly the active site, it is not obvious which portion of the dimerized pyrimidines, if any, stick into the cavity, or if the dimer is in vdW contact with the FAD at the base of the hole. Another DNA repair enzyme, T4 endonuclease V, is known to flip out an adenine that is opposite a thymidine dimer in order to gain access to the dimer itself (*16*). Studies using alanine mutants strongly suggest that the dimer flips out of the DNA duplex directly into the cavity where it appears to be in close contact with several aromatic residues (*17*). The significance of these interactions are not fully understood but may involve both substrate positioning by the protein as well as protein-mediated electron transfer from the $^1FADH^-$ to the T<>T lesion.

An apparently unrelated observation of protein−substrate *electronic* interactions was that of a blue-shifted absorption spectrum of the folate-depleted *oxidized* photolyase−substrate complex obtained by Jorns et al. (*1*). We reasoned that this spectral shift could be the result of two possible scenarios: either a conformational change in the protein upon substrate binding that perturbs the electrostatic environment of the flavin cofactor or an electrochromic shift in the flavin absorption spectrum due to the presence of the dipolar thymidine dimer substrate.

If the spectral shift was due to protein−FAD interactions, then we would expect aromatic residues to be involved (although movement of a charged residue is also possible). Similar spectral changes have been noted in riboflavin-tryptophan complexes more than 50 years ago (*18*). These interactions are known to have a effect on the lifetime of the singlet excited states of the flavin, as we have shown previously using femtosecond transient absorption spectroscopy (*19*). It is known from the crystal structure of the enzyme that there are several tryptophan residues that are close to either the flavin and/or adenine rings (e.g., Trp 277, 382, and 384) that might provide the appropriate electronic perturbation. Such a perturbation might manifest itself as a shortened excited-state lifetime. We report on such measurements in this communication.

The possibility that the substrate might be responsible for the blue shift in the absorption spectrum is based on the realization that the cyclobutylthymidine dimers have a relatively coplanar geometry that would essentially double the already substantial permanent dipole moment of the thymidine base [∼4 D (debye) (*20*)]. This dipole moment would produce a dipolar electric field that would fall off as $1/r^3$. If the CPD dipolar electric field were inducing an electrochromic shift, then the relative orientation of the dimer dipole moment and FAD *difference* dipole moments would be crucial in determining the direction of the shift. The magnitude of the shift would also depend on the magnitude of the dimer electric field experienced by the FAD cofactor inside the substrate cavity. We have made a simple calculation of the spectral shift based on this hypothesis, which is consistent with Stark spectroscopic measurements made in our laboratories (*21*). The implications of this model for electron-transfer-mediated repair are outlined below.

MATERIALS AND METHODS

Protein Preparation. Photolyase was overexpressed in JM109 *E. coli* using the pMS969 plasmid, which was a generous gift from Aziz Sancar (*22*). The cells were grown in terrific broth [12 g of tryptone (Fisher), 24 g of yeast extract (Fisher), 4% glycerol, 2.31 g of KH_2PO_4, and 12.54 g of K_2HPO_4/L] and induced with IPTG (Fischer) when the optical density at 600 nm was ∼0.6 OD as measured by a Hewlett-Packard 8452A UV−vis Spectrophotometer. Three hours after induction the cells were spun down at 10000*g* for 10 min, resuspended in 20 mL of lysis buffer (50 mM potassium phosphate, 100 mM NaCl, 1 mM EDTA, 10 mM 2-mercaptoethanol, and 1 mg/mL benzamidine, pH 8.0), and frozen at −80 °C.

For protein preparation, ∼15 g of frozen cells was thawed on ice in the presence of lysozyme (1 mg/mL). After sonicating with eight 30 s bursts at 25 W, with 30 s between bursts, the cell lysate was spun for 30 min at 30000*g* and the pellet discarded. The supernatant was again spun for 1 h at 120000*g*. The supernatant from this high-speed centrifugation was subjected to a two-step ammonium sulfate (AS) precipitation. After adding saturated aqueous AS to 40% concentration, the mixture was stirred slowly for 1 h at 4 °C, then centrifuged for 20 min at 10000*g*. The supernatant was poured off and brought to 75% AS concentration, allowed to stir 1 h at 4 °C, and spun down at 10000*g* for 20 min. The pellet was resuspended in 10 mL of buffer B (50 mM potassium phosphate, 20 mM KCl, 1 mM EDTA, 10 mM 2-mercaptoethanol, 20% glycerol, pH 7.4) and dialyzed overnight in 4 L of buffer B. After dialysis, the protein was loaded onto a 30 mL blue sepharose 6 fast flow column (Pharmacia) and rinsed with 1 mM ATP in buffer B until the absorbance at 280 nm leveled off, then eluted with a KCl gradient from 20 mM to 2 M. The protein eluted at ∼360 mM KCl concentration.

The apoprotein and reconstituted photolyase were prepared using a slightly modified procedure of Jorns et al. (*1*). To prepare the apoprotein, holoenzyme of at least 75% purity was diluted 4-fold with buffer apo-A (50 mM potassium phosphate, 1.7 M ammonium sulfate, 0.5 mM EDTA, 10 mM 2-mercaptoethanol, 20% glycerol, pH 7.0) and loaded onto a 10 mL phenyl sepharose-6 fast flow, high sub column (two Pharmacia Hi-Trap columns linked in tandem). Purity was determined by comparing the measured ratio of absorbance at 280 and 580 nm to a theoretical value arrived at by using $\epsilon^{280} = 128\,000\ M^{-1}\ cm^{-1}$ and $\epsilon^{580} = 4800\ M^{-1}\ cm^{-1}$. After loading and rinsing with buffer apo-A, chromophores were stripped from the photolyase by rinsing with apo-B (50 mM potassium phosphate, 1.7 M ammonium sulfate, 0.5 mM EDTA, 10 mM, 2-mercaptoethanol, 20% glycerol, saturated KBr, pH 3.5). The column was then reequilibrated in apo-A, and the apophotolyase was eluted with apo-C (100 mM potassium phosphate, 0.5 mM EDTA, 10 mM 2-mercaptoethanol, 50% ethylene glycol, pH 7.0).

The apoenzyme was incubated overnight in a 100-fold excess of FAD (ICN Pharmaceuticals), then diluted 10-fold with apo-A and loaded back onto the phenyl sepharose column. After thoroughly rinsing with apo-A, the reconstituted protein was eluted with buffer T (50 mM potassium phosphate, 0.1 mM EDTA, 10 mM 2-mercaptoethanol, 5% glycerol, pH 7.5). Buffer T is storage buffer prepared with low glycerol to facilitate centrifugal concentration (30k molecular weight cutoff centrifugal concentrator Amicon Ultrafree). Glycerol was added to 30%, the sample was flash-frozen in liquid N_2 and stored at −80 °C. Quantitation of the reconstituted protein concentration was measured by absorption spectroscopy using an extinction coefficient of $\epsilon_{443} = 11\,200\ M^{-1}\ cm^{-1}$ for the FAD chromophore in photolyase (*1*). The entire purification procedure took place under yellow light between 4° and 10 °C.

Substrate Preparation. Single-stranded (ss) DNA substrate was prepared from both 2-mer and 18-mer thymidylic acid. The procedure for dimerizing the dinucleotide was as follows: 20 units of $d(pT)_2$ (Sigma) was dissolved in 75 mM phosphate buffer, 10% acetone, pH 6.8, and de-oxygenated with argon in a 1 cm path-length fused silica fluorescence cuvette. The DNA was then irradiated on ice through a polystyrene Petri dish for 3 h using two 40 W UVB lights (Phillips TL-40) at a distance of 6 cm. The irradiated DNA was desiccated in a Speed-Vac (Savant SC-110) and resuspended in 100 μL of HPLC-grade water and injected onto a Waters C_{18} HPLC column in a mobile phase consisting of 75 mM phosphate, pH 6.8 at 1 mL/min. The CPD dimers did not adhere to the column and were collected, desiccated, and desalted by reinjection onto the same column in a mobile phase of pure water. The final product was dried and stored at −20 °C. Unreacted starting material was recovered from the column with a 0.5%/min acetonitrile gradient, desiccated, and stored at −20 °C.

Polymeric DNA substrate was prepared from $d(pT)_{18}$ (Sigma) by irradiating as described above, then desalted on a Bio-Rad Micro-Bio Spin 6 column, desiccated, and stored at −20 °C.

Both substrates were assayed for repair activity using 3 μM reconstituted photolyase in assay buffer (50 mM potassium phosphate, 0.1 mM EDTA, 10 mM 2-mercaptoethanol, 30% glycerol, 200 μM DTT, 20 μM sodium dithionite, pH 7.5) in a 3 mm path-length fused silica cuvette fitted with a septum. Prior to irradiation, the cuvette was purged with argon. The protein was photoreduced on ice with 365 nm light from a Spectraline ENF-240C hand lamp (4 W) at a distance of 2 cm. The spectrophotometer was blanked against the assay mixture and dimerized DNA was then added to give an A_{265} value between 0.5 and 0.75 OD. After saving this spectrum, the instrument was blanked again versus the assay mixture and the sample was irradiated with the hand lamp until the peak at 265 nm ceased to rise.

Steady-State UV−Vis Absorption Spectroscopy. Most steady-state absorption measurements were performed using an HP 8452A photodiode array spectrometer. This instrument has a band-pass of 2 nm. For more accurate determinations of the maxima in absorption spectra, we used a setup similar to that described in our Stark spectroscopy work (*21*). Briefly, a 150 W Xe arc lamp was spectrally filtered through a $^1/_8$ m monochromator with a band-pass of 0.5 nm. The monochromatic light was directed through a chopper operating at ∼2.7 kHz and subsequently passed through the sample cell, typically a 1 mm fused silica cuvette. The transmission changes for both the reference buffer and the sample were detected by a silicon photodiode and measured using a lock-in amplifier.

Transient Absorption Spectrometer. Transient absorption data was acquired using a Ti:sapphire-based femtosecond transient absorption spectrometer described previously (*19*) except as modified below. The photolysis pulse was generated by frequency doubling the 780−800 nm output of the laser with a 2 mm thick type-I BBO crystal, which produced an ultraviolet pulse with a bandwidth of about 2 nm. After doubling, the photolysis pulse was bounced off an aluminum-coated hollow retroreflector which was mounted on a motor-driven translation stage with a 3 ns range and 6 fs resolution (Aerotech). A logarithmic time scale was used as it provides many data points at early times to resolve fast decay rates and fewer points at later time to facilitate averaging by reducing the duration of each scan.

Residual 780 nm light was removed by a Schott BG 38 filter, and the beam fluence was adjusted using a Glan-Thompson polarizer. The relative polarization of the pump and probe pulses was set to the magic angle by a UV-half wave plate. The photolysis pulse was chopped (New Focus 1340) at half the repetition rate of the probe pulse. The photolysis pulse was focused onto the sample with a 20 cm focal length parabolic reflector and subsequently blocked.

Single-frequency probe pulses at the same wavelength as the photolysis pulse were generated by splitting off a small portion of the photolysis pulse after the red-blocking filter with an uncoated fused silica flat. Alternatively, a white light continuum was generated by splitting off ∼10 μJ from the fundamental beam using a fused silica flat, which was attenuated by a variable neutral density filter before focusing with a 10 cm lens onto a 2 mm crystal quartz window. Emerging continuum light was collimated by a 5 cm focal length off-axis parabola (Janos Technologies). The probe pulse was then sent along a fixed-length delay, made parallel to the pump beam, and focused onto the sample by the same parabolic reflector as the pump beam.

The protein solutions were held in spinning fused silica cell with a 1″ in. aperture and a 1.6 mm path length. The sample cell was constructed in-house from two optical flats separated by a buna O-ring. The parallelism of the flats was maintained by six adjustable bolts in an aluminum annular ring. The ring assembly was mounted in a pillow-block (Fafnir) on a translation stage the motion of which was adjustable parallel to the beam axis. The cell was spun by a dc motor (Pittman Lo-Cog) using a rubber belt at sufficient speed to ensure that the sample was replaced between each shot (∼35 Hz). Measurements were carried out at room temperature.

After the probe beam passed through the sample, it was apertured to remove scattered light from the pump beam, recollimated by a 20 cm focal length plano-convex quartz lens, and focused by a 3 mm focal length achromat into a $^1/_8$ m monochromator (CVI Laser CM110SP) with a 0.15 mm entrance slit, and a 2.4 mm exit slit (∼8 mm band-pass). Upon exiting the monochromator, the beam was focused onto a 400 MHz UV-enhanced silicon diode (Thor Labs DET 210).

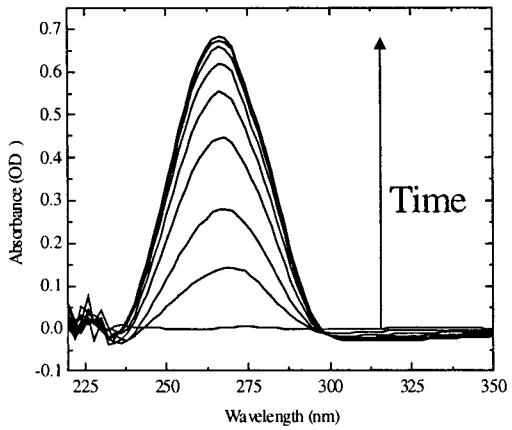

FIGURE 1: Reactivation of UV-irradiated d(pT_2) by dithionite-reduced *E. coli* DNA photolyase using 365 nm light. The lowest trace is the spectrum of the assay mixture before exposure to 365 nm light. Subsequent spectra are the result of 5 min periods of exposure to the reactivating light. The concentration of photolyase was 5 μM while the concentration of substrate is 40 μM.

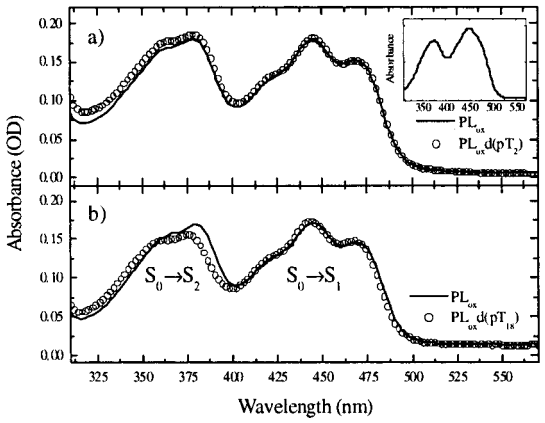

FIGURE 2: UV−vis spectra of the enzyme−substrate complexes. The path length was 1 mm for both panels. The spectra are normalized to the peak absorbance at 444 nm. (a) Spectrum of PL_{ox} with (−) and without (○) d(pT_2) dimer substrate. The electronic transition is indicated under each absorption band. The concentration of enzyme is 150 μM with a 20-fold excess of d(pT_2). No band shifts were observed. (b) Spectrum of PL_{ox} with (−) and without (○) d(pT_{18}) dimer substrate. The enzyme concentration was 150 μM with a substrate concentration of ∼300 μM in dimer. Both $S_0 \rightarrow S_1$ and $S_0 \rightarrow S_2$ bands are blue shifted relative to the enzyme-only spectrum.

The output of the photodiode was amplified (Mini-Circuits ZFL-1000) and fed into two boxcar integrators (SRS 250). The "reference" boxcar was gated at 500 Hz to measure the probe beam signal when the photolysis beam was blocked by the chopper while the "signal" boxcar measured changes in the transmission of the probe pulse at 1000 Hz. The reference boxcar was set to average the input to provide the transmission I_0 while the output of the signal boxcar (no averaging) was fed into a lock-in amplifier (SRS 810) to obtain the difference in transmission due to photolysis (ΔI). ΔI was calculated taking into account the duty cycle of the "square wave" output of the signal boxcar. The degree of averaging of the reference boxcar was set to take advantage of the lock-in time constant. The lock-in amplifier was also used to digitize the reference output using one of four 16-bit analogue to digital converters in the unit. This information was processed by in-house written Labview software on a Pentium-based computer to obtain the normalized absorbance change, $\Delta A = \log(I_0/\Delta I)$.

The instrument response function was generated by measuring a Kerr-effect lens in the sample cell filled with buffer T. For white-light continuum scans, the chirp on the pulse was determined by measuring the time delay between the maxima of the Kerr lens over the range of wavelengths studied. The photolysis pulse energy was measured with a joulemeter (Molectron J3S-10) after reflection off a 3° quartz wedge and attenuation through a neutral density filter.

RESULTS

Photoreactivation of Substrates by Photolyase. A 1 mL assay solution of 3−5 μM dithionite-reduced photolyase and 40 μM of dimerized d(pT)$_2$ was prepared as described above, and the UV−vis spectrometer was blanked against this mixture. Immediately thereafter, a spectrum was taken and labeled as "zero minutes", and subsequent spectra were measured at 5 min intervals after irradiation with 365 nm reactivating light. Reconstruction of the vinyl bonds in thymidine accounts for the increasing absorbance at 265 nm which have a molar extinction coefficient of ca. 9500 M^{-1}/bond or 19 000 M^{-1}/dimer (*23*) as seen in Figure 1. Repair was initially linear with time, but leveled off as the substrate was repaired. Similar results were obtained with 18-mer substrate, but with a rate approximately 15 times as fast (data not shown).

Spectral Shift Measurements. The UV−vis absorption spectra of PL_{ox} with and without substrate were taken at 150 μM in enzyme. The enzyme without substrate (−) is shown in both panels of Figure 2 to facilitate comparison with the enzyme−substrate spectra. The spectral region depicted in the figure corresponds to the $S_0 \rightarrow S_1$ (∼444 nm) and $S_0 \rightarrow S_2$ (∼380 nm) transitions of the FAD cofactor. Vibronic bands are well resolved, which is indicative of tight binding between the noncovalently bound FAD and the highly ordered protein structure, as well as the nonpolar nature of the flavin binding pocket. The inset in Figure 2a shows the corresponding spectrum of FAD in aqueous solution at neutral pH. Vibronic structure is no longer apparent because numerous available orientations of water molecules about the chromophore create a distribution of ground-state energies with concomitant smearing of vibronic structure.

A blue shift in the absorption spectrum was evident upon binding of dimerized 18-mer oligothymidylic acid [d(pT)$_{18}$] by Pl_{ox} (O, Figure 2a), as was previously observed by Jorns et al. (*1*). The shift was significantly larger for the 380 nm band than for the 444 nm band. Higher resolution measurements of the spectral shifts were performed as described above (0.5 nm band-pass). Peaks were assigned where the first derivative of the absorption spectrum equaled zero and the second derivative was negative [as calculated numerically using MATLAB 6.0 (the Mathworks)]. Quantification of the blue shift was accomplished by converting the wavelength scale of the absorption spectrum to wavenumbers and subtracting the energies of the peak transitions with and without substrate for each of the two absorption manifolds ($S_0 \rightarrow S_1$ and $S_0 \rightarrow S_2$). This procedure yielded values of 88 cm^{-1} (1.7 nm) for the $S_0 \rightarrow S_1$ transition and 325 cm^{-1} (4.6 nm) for the $S_0 \rightarrow S_2$ transition. Thus, the shift at 380 nm is about 3.7 times larger than at 444 nm. In addition there appears to be a small loss of oscillator strength for the $S_0 \rightarrow$

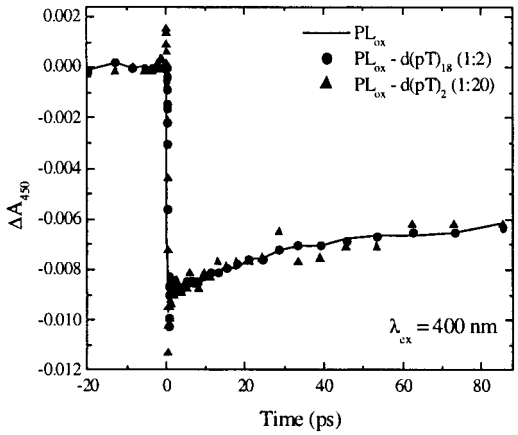

FIGURE 3: Transient absorption decays of PL_{ox} (−), PL_{ox}-d(pT_{18}) (●), and PL_{ox}-d(pT_2) (▲), where the substrates include a CPD. The probe wavelength was 450 nm. The cross correlation width for these measurements gives a full width at half-maximum response of about 400 fs, as measured using the optical Kerr effect in the sample cell filled with buffer T.

S_2 transition relative to the $S_0 \rightarrow S_1$ transition when bound to substrate.

In contrast, no shift of the absorption spectrum was observed when dimerized dithymidylic acid [d($pT)_2$] was used as a substrate (Figure 2b), despite the fact that both undergo repair as evidenced by the reactivation assays. The small offset in absorbance observed upon addition of the dithymidylic substrate is most likely due to increased light scattering. The difference in the singlet transition energies for photolyase bound to dimeric or polymeric ss-DNA suggests significantly different binding orientations for these two substrates.

Time-Resolved Spectroscopy. Previous work in this laboratory (*19*) and others (*24*−*28*) have demonstrated that significant excited-state quenching of flavins occurs when electron-rich (aromatic) molecules are brought into vdW contact with the isoalloxazine ring. The crystal structure of photolyase shows that tryptophans 277, 338, 366, 384, and 382, as well as phenylalanine 366 are within a few angstroms of FAD. Intramolecular quenching by adenine (*24*) is also a possibility, as the ribityl tether loops around to bring the adenine very close to the isoalloxazine moiety, a configuration which is unique among all flavoproteins observed to date (*15*). In response to these issues we performed time-resolved transient absorption measurements to determine whether the spectral shift could be correlated with excited-state quenching. If so, this would indicate that a conformational change occurs upon substrate binding that alters the local environment of the FAD.

Subpicosecond decay kinetics for oxidized photolyase have not been reported previously. The oxidized enzyme was used to study the enzyme−substrate complex without the complication of CPD repair. Single wavelength kinetics of the excited-state decay of the oxidized enzyme probed at 450 nm with excitation at 400 nm over 85 ps is shown in Figure 3 (−). In addition, the decay kinetics of PL_{ox} with the two different substrates are also plotted. At this wavelength, we are probing the ground-state bleach of the $S_0 \rightarrow S_1$ transition. The addition of two equivalents of 18-mer oligothymidylic acid with an average of 1.8 T<>T lesions per strand (●) or 20 equiv of d($pT)_2$ (▲) produced no difference in the decay

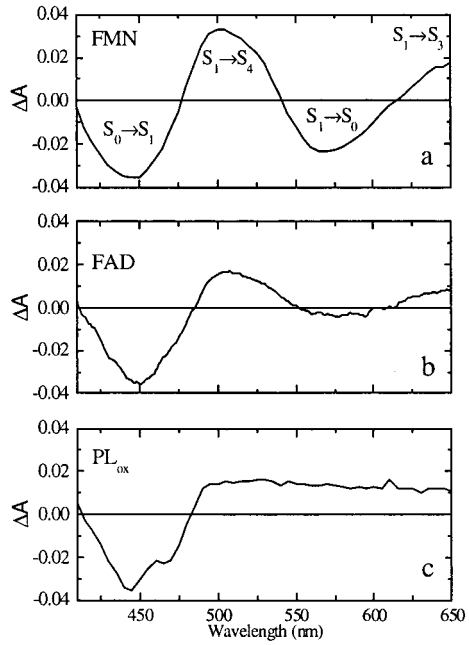

FIGURE 4: (a) Transient absorption spectrum of 250 μM FMN in water, taken 5 ps after excitation with 396 nm light. The panel is annotated with the putative assignments. See the text for a description of these assignments. (b) Transient absorption spectrum for FAD in water at 5 ps with excitation at 396 nm. Excited-state quenching is evident by comparing the 570 nm region in this spectrum and that of FMN. The quenching is ascribed to base stacking between the isoalloxazine and adenine rings and may involve charge transfer. (c) Transient absorption spectrum of DNA photolyase at 5 ps, taken with 400 nm excitation. The ground state bleach centered around 445 nm shows the same vibronic structure seen in the steady state absorption spectrum. No stimulated emission is seen, only a broad absorption above 490 nm. Similar behavior in the transient absorption of flavoproteins has been ascribed to the formation of a charge transfer complex between the isoalloxazine and an aromatic amino acid residue. In DNA photolyase, the charge transfer donor is likely to be the adenine ring.

kinetics. The decay in all cases is single exponential within the signal-to-noise, giving a time constant of about 30 ps. However, this is due to the small time range used to monitor the excited-state decay. Data taken over a longer time range showed that the bleach persists for more than 300 ps but did not reveal a dependence on either substrate (data not shown). Measurements taken with and without substrate at other probe wavelengths (530 nm, 590 nm) are also indistinguishable within experimental error (data not shown). These same samples were used to obtain the steady-state spectra in Figure 2, panels a and b. These data show that the structure of the protein around the FAD-binding site does not change very much due to substrate binding.

Transient spectra from 410 to 650 nm were obtained using a white light continuum probe at 5 ps after excitation to gain a better understanding of how the protein interacts with the FAD cofactor. To fully appreciate these data, it is useful to review what has been learned about the excited state of flavins in aqueous solution (*19*). We begin by examining the transient absorption spectrum of FMN in water at neutral pH.

The transient absorption spectrum of FMN (250 μM) at 5 ps using 396 nm excitation is shown in Figure 4a. We and others have assigned the transient absorption spectra of the free oxidized flavins (*19*, *27*, *29*). The region of negative

absorbance centered around 450 nm is a ground-state bleach of the strong $S_0 \rightarrow S_1$ band. Flanking the ground-state bleach are regions of positive absorbance (e.g., ~650 and ~505 nm) which have been assigned to excited-state absorption from $S_1 \rightarrow S_3$, S_4, etc. The negative absorption band at 570 nm has been assigned to stimulated emission from $S_1 \rightarrow S_0$. Flavins in aqueous solution usually have a fluorescence maximum around 520 nm but this emission peak is buried under the intense excited-state absorption band at 505 nm. The excited-state features have a lifetime of several nanoseconds for FMN.

The transient absorption spectrum of aqueous FAD (Figure 4b) shows much the same spectral signature as FMN at 5 ps except that the features are attenuated due to excited-state quenching of the S_1 state by intramolecular (dynamic) base stacking of the adenine and isoalloxazine rings (*19*). It has been estimated that the dynamic nature of this stacking interaction leads to a 90% fraction of FAD molecules in a base stacked (quenching) configuration in aqueous solution (*25*). A result of base stacking is the relative loss of the stimulated emission band compared to the 505 nm band. This can be ascribed to a charge-transfer band competing for absorbance in this spectral region. Transient absorption in this 520−600 nm region has also been assigned to charge-transfer activity in flavin−indole complexes (*24*, *30*, *31*) and other flavoproteins (*27*, *32*).

The transient absorption spectrum of DNA photolyase is markedly different from those of flavins in simple solvents (Figure 4c). Excitation energy was 900 nJ/pulse at 400 nm with a cross correlation width of 400 fs full width at half-maximum. Spectral features at 415, 445, and 465 nm correspond to the vibronic structure of the ground-state absorption spectrum. A more significant difference between PL_{ox} and simple flavins is the broad absorption from 490 to beyond 650 nm, which is indicative of charge transfer between the FAD and some electron donor in the protein. The decay kinetics of PL_{ox} are intermediate between FMN(aq) and FAD(aq) (*19*), suggestive of some quenching due to the protein, however, the transient absorption spectrum of PL_{ox} does decay slowly over a few nanoseconds (data not shown). Thus, the protein is designed to sustain the optical excitation of the FAD, but charge transfer may play a role in facilitating the electron-transfer reaction.

Substrate Electrochromism in PL_{ox}. Time-resolved spectra of Pl_{ox} show no measurable difference in decay rates between the free and substrate-bound enzyme. This result implies that no conformational change occurs in the protein which would bring aromatic amino acid residues closer to FAD, since excited state quenching would be expected if electron-rich orbitals were brought into vdW contact with the flavin moiety. In addition, our experiments effectively eliminate the possibility that direct orbital contact occurs between dimer and cofactor by the same argument. This conclusion is corroborated by many computational studies that show the dimer−cofactor distance to be anywhere from 3 to 22 Å (*33*−*35*). At first glance, this would appear to be at odds with the observed blue shifting of the spectrum upon binding oligomeric substrate, but the spectral shift need not be caused by something adjacent to the FAD cofactor. Spectral band shifts can be brought about by changes in the electric field around the chromophore (*36*). Since no rearrangement of the protein matrix was observed in the time-resolved data, we hypothesize that the band shifts (~88 cm^{-1} for $S_0 \rightarrow S_1$ and ~325 cm^{-1} for $S_0 \rightarrow S_2$) are due to an electric field from the dipolar thymidine dimer. Thymine has a dipole moment of about 3.9 D (*20*, *37*), and the two nucleotides comprising the dimer are thought to be in a nearly coplanar arrangement (*4*). If this large dipole moment points in the appropriate direction relative to the FAD cofactor, then the resultant electric field would be sufficient to account for the blue shifts observed in both transitions. Interestingly, Berg and Sancar (*17*) suggested that a glutamic acid residue at the base of the binding cavity (Glu^{274}) might direct the electron from the $^1FADH^-$ to the CPD, but the charged residue cannot explain the spectral shift we and others have observed. This residue is about 9 Å from the isoalloxazine structure and would have to shift it's position by more than 2 Å in order to produce the measured shift, assuming a dielectric constant of 6. This seems unlikely, as the transient absorption data offered no indication of a major conformational change in the protein upon substrate binding.

The theory of electrochromism (*36*) requires that the band shift (ΔE, in cm^{-1}) be proportional to the (dipolar) electric field of the CPD and the difference dipole moment of the chromophore:

$$\Delta E = \frac{-\Delta\vec{\mu}_n^{FAD}\cdot\vec{F}_{CPD}}{hc} = \frac{-|\Delta\vec{\mu}_n^{FAD}||\vec{F}_{CPD}|\cos\gamma}{hc} \quad (1)$$

where $\Delta\vec{\mu}_n^{FAD}$ is the difference dipole moment for the flavin cofactor ($\Delta\vec{\mu}_n^{FAD} = \vec{\mu}_n - \vec{\mu}_0$, where n is the index of the transition from the ground (0th) state to the nth excited singlet state), $\vec{F}_{CPD}$ is the electric field at the cofactor due to the CPD, γ is the angle between these two vectors, h is Planck's constant, and c is the speed of light. One compelling reason to believe that electrochromism is at play in this system is the recent Stark spectroscopic measurement of $\Delta\vec{\mu}_n^{FAD}$ (n = 1, 2) for *N*(3)-methyl-*N*(10)-isobutyl-7,8-dimethylisoalloxazine in simple solvents (*21*). The ratio of difference dipole moments from this work is $\Delta\vec{\mu}_2^{FAD}/\Delta\vec{\mu}_1^{FAD} = 3.0 \pm 0.1$. This is close to the ratio of the spectral shifts observed herein, $\Delta E_2{:}\Delta E_1 \approx 3.7$. If the spectral shifts are due to electrochromism, then the calculation of $\vec{F}_{CPD}$ from the spectral shifts and Stark parameters would be constrained in several ways. For example, γ must be greater than 90° to produce a blue shift. This requirement in turn places geometric constraints on the orientation of the dimer in the protein and its distance from the FAD cofactor. To place this hypothesis on a more quantitative basis, we begin by estimating the dipole moment of the CPD. To this end, we start with an approximate structure of the FAD-CPD system, as provided by a recent molecular dynamics simulation of Sanders and Wiest (*34*). The calculation of $\Delta\vec{\mu}_n^{FAD}$ for these models is described in Appendix 1.

Two models of photolyase docked with a 9-mer of single-stranded DNA were offered by Sanders and Wiest, one with the single strand of DNA holding the conformation it would have if it were joined to a complementary strand by Watson−Crick base pairing (B-DNA form), and one in which the dimer was rotated from its usual position into the protein cavity ("flipped out") (*34*). Figure 5, panels a and b, shows the "flipped out" and normal ("not flipped") cofactor−substrate orientations, respectively; we present these models

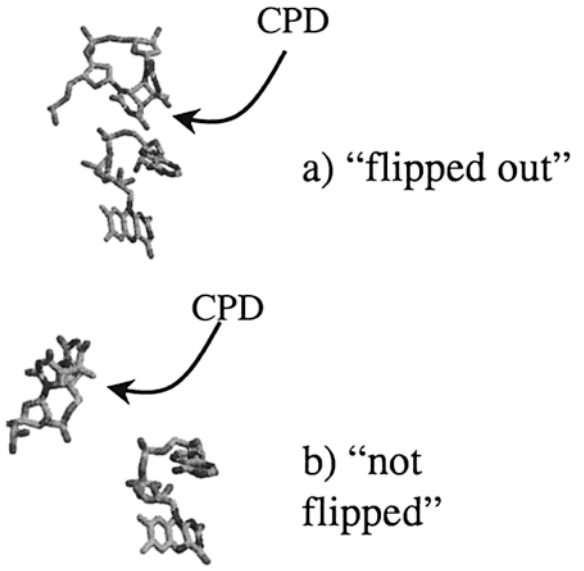

FIGURE 5: (a, b) Geometry of FAD and CPD in the "flipped out" and "not flipped" conformations, as taken from the simulations of Sanders and Wiest (*34*). The CPD cyclobutane ring can be seen most clearly in panel a as a square separating the thymidine bases. Hydrogens, protein, and DNA backbone have been omitted for clarity.

to clarify the discussion below. Partial charges were assigned using the results of Hahn et al. (*33*), and these were used to compute $\vec{\mu}_{CPD}$ for Sanders and Wiest's models as described below.

The CPD dipole moment direction can be visualized by imagining a vector normal to the cyclobutane ring which points away from the coplanar thymine rings. The calculated value of the dipole moment, $\vec{\mu}_{CPD}$, is slightly different for each of the models due to variations in the CPD's conformation, but were all within a range of 7.4 ± 0.3 D. This is in good agreement with density functional calculations (*38*), which gives a value of 7.0 D, and the 6.85 *D* value for the *cis-syn* uracil dimer from the ab initio calculations of Voityuk and Rösch (*39*).

Calculation of the CPD Dipolar Electric Field, $\vec{F}_{CPD}$. $\vec{F}_{CPD}$ will be a function of the direction and magnitude of the CPD dipole,$\vec{\mu}_{CPD}$, as well as its orientation and distance relative to the FAD cofactor. The electric field produced by a point dipole is (*40*)

$$\vec{F}_{CPD} = \left(\frac{1}{4\pi\epsilon\epsilon_0}\right)\left[\left(\frac{3(\vec{\mu}_{CPD}\cdot\vec{r})\vec{r}}{|\vec{r}|^5}\right) - \left(\frac{\vec{\mu}_{CPD}}{|\vec{r}|^3}\right)\right] \qquad (2)$$

where $\vec{r}$ is a vector pointing from the CPD dimer C5 to the isoalloxazine moiety N10, $\vec{\mu}_{CPD}$ is the permanent ground-state dipole moment of the thymidine dimer, $\epsilon_0 = 8.85 \times 10^{-12}$ C^2 J^{-1} m^{-1}, and ϵ is the effective dielectric constant. $\vec{\mu}_{CPD}$ was calculated by assigning partial charges reported by Hahn et al. (*33*) to the appropriate coordinates from the .pdb files kindly provided by Dr. Wiest, and summing these charges by the distance to the center of coordinates given in the .pdb file. Only atoms on the thymine rings were used; no attempt was made to account for the DNA backbone. This may seem to be a significant omission, as the negatively charged phosphates comprising the backbone generate a point-charge field that falls off as $1/r^2$, as compared to $1/r^3$ for a dipolar field. However, these phosphates are predominately neutralized by positively charged amino acid residues in the binding cleft. Also, if these phosphates were responsible for the spectral shift then this shift should also appear for high concentrations of undimerized DNA, as it is weakly bound by the protein. No such behavior has been reported. Indeed, our experiments have been performed in 50 mM phosphate buffer which would saturate the surface of the protein with negative phosphate groups.

Table 1: Electrochromic Model Parameters ($\epsilon = 1$)

	flipped out	not flipped	dinucleotide	"best fit"
$\lvert\vec{F}_{CPD}\rvert$ (V/m)	8.1×10^7	3.6×10^7	1.2×10^8	2.7×10^8
γ_1 (deg)	173	127	92.1	141
γ_2 (deg)	112	168	73.4	165
ΔE_1 (cm^{-1})	33.7	7.7	1.5	325[a]
ΔE_2 (cm^{-1})	38.6	38.0	−37.0	88[a]
$\Delta E_2/\Delta E_1$	1.1	4.9	−24.7	3.7[a]

[a] These values were constraints of the model.

Electrochromic Model Calculations. The results of the electrochromic model calculations are summarized in Table 1. $|\vec{F}_{CPD}|$ is the dipolar electric field strength at the FAD cofactor. γ_1 and γ_2 refer to the angle between $\Delta\vec{\mu}_1^{FAD}$, $\vec{F}_{CPD}$ and $\Delta\vec{\mu}_2^{FAD}$, $\vec{F}_{CPD}$, respectively, calculated for the models described above. It should be noted that the angle cited is the included angle and may not necessarily lie in the plane of the flavin ring. The electrochromic shifts for these values are given as ΔE_1 and ΔE_2 for the two electronic transitions; a positive value corresponds to a blue spectral shift.

For the d(pT$_{18}$) substrate, $\vec{\mu}_{CPD}$ produced an electric field that was nearly coplanar with the isoalloxazine plane, whether the CPD was "flipped out" or "not flipped". Given the 3:1 ratio of $\Delta\vec{\mu}_2^{FAD}$:$\Delta\vec{\mu}_1^{FAD}$ determined by Stark spectroscopy, it is apparent that the CPD's electrostatic field has to be better aligned with $\Delta\vec{\mu}_2^{FAD}$ than $\Delta\vec{\mu}_1^{FAD}$ in order to produce the ratio of 3.7 obtained from the observed shift.

For the "not flipped" (B-DNA) conformation our calculations indicate that the angle between $\Delta\vec{\mu}_1^{FAD}$ and $\vec{F}_{CPD}$ would be $\gamma_1 = 127°$ with a field strength of 3.6×10^7 V/m if the intervening space is devoid of dielectric material. This produces a blue shift of about 8 cm^{-1}, much less than the observed 88 cm^{-1} shift. Similarly, for the $\Delta\vec{\mu}_2^{FAD}$ difference dipole moment an angle of $\gamma_2 = 168°$ was obtained with a blue shift of 38 cm^{-1}, about a factor of 9 less than the 325 cm^{-1} shift observed. The ratio of shifts is 4.9, too large compared with the experimentally determined value of 3.7. These results suggest that both the orientation of the CPD is incorrect and the distance is too large (15 Å) to be explained by the electrochromic model.

A field strength of 8.1×10^7 V/m was produced by the "flipped out" dimer. γ_1 and γ_2 are 173° and 112°, respectively. The shifts for these parameters are 34 and 39 cm^{-1} for band I and band II, respectively, and their ratio is 1.1. Neither the absolute magnitude of the calculated shifts nor their ratio agree well with the observed values. Therefore, we reach the conclusion that neither substrate docking model accurately reflects the appropriate orientation and distance to be explained by the electrochromic model.

In contrast to the polynucleotide substrate, calculations for the dinucleotide substrate yielded a field strength of 1.2×10^8 V/m, with the field direction significantly out of the isoalloxazine plane. γ_1 and γ_2 are 92° and 73°, respectively,

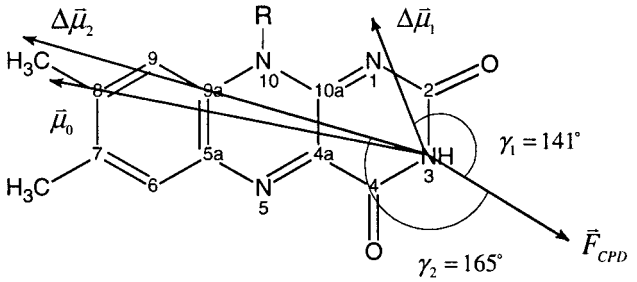

FIGURE 6: Orientation of the substrate electric field, $\vec{F}_{CPD} = 2.7 \times 10^8$ V/m, to the difference dipole moments of the FAD in photolyase, $\Delta\vec{\mu}_n^{FAD}$ for $\epsilon = 1$. The dimer substrate was oriented so that $\vec{F}_{CPD}$ is in the plane of the flavin and the electrochromic shift produced by this field and $\Delta\vec{\mu}_1^{FAD}$ and $\Delta\vec{\mu}_2^{FAD}$ matches the observed shift. The angles between the difference dipole moments come from Stark spectroscopy measurements (*21*). $\vec{\mu}_0^{FAD}$, which is roughly parallel to $\vec{m}_I$, is shown for reference.

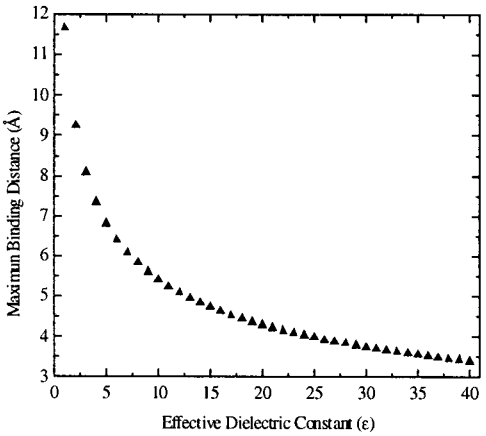

FIGURE 7: Binding distance of the d(pT_{18}) CPD to the FAD in photolyase vs the effective dielectric constant, as predicted by the "best fit" electrochromic shift model.

with the calculated shifts being 1.5 and -37 cm^{-1} for band I and band II, respectively. Thus, we expect a red shift of the S_2 band and a negative $\Delta E_2/\Delta E_1$ ratio, neither of which was observed. It is possible that the dinucleotide substrate is bound by only a single phosphate and only occasionally binds in the catalytic pocket. In this case, no spectral shift would be observed, as the spectrophotometer would measure an average of all available binding configurations.

Conversely, we can use the measured-shift ratio to calculate the required angle between $\vec{F}_{CPD}$ and $\Delta\vec{\mu}_n^{FAD}$, in the sense that the calculated angle and field strength produce the observed blue shifts and shift ratio. There is a strong directional dependence to the magnitude of a dipolar electrostatic field, which is greatest in the direction of the dipole moment, so the largest electrochromic shift would occur when $\vec{\mu}_{CPD}$ points directly at the flavin and in the flavin's plane. This enables us establish a maximum separation between isoalloxazine and the dimer as a function of the effective dielectric constant of the protein that are consistent with the spectral data. The details of this "best fit" calculation can be found in Appendix 2.

This "best fit" model is essentially two bare dipole moments, devoid of material structure, embedded in a continuum dielectric. As such, it represents the electrochromic hypothesis in its simplest construction. Bearing this in mind, the magnitude of the measured blue-shift requires an electrostatic field strength of 2.7×10^8 V/m for $\epsilon = 1$ with $\gamma_1 = 141°$ and $\gamma_2 = 165°$. The relationship between this substrate electric field and the difference dipole moments is shown schematically in Figure 6. This field defines a maximum distance for which even a perfectly aligned dipole field could produce the measured shift, ~12 Å. If the field passes through anything but vacuum, the field strength is reduced by dielectric shielding, requiring a closer docking distance. To examine this, $\vec{\mu}_{CPD}$ was varied in distance along the direction corresponding to $\gamma_1 = 141°$ and $\gamma_2 = 165°$, and electrochromic shifts were calculated according to eqs 1 and 2 for permittivity values ranging from 1 to 40. The maximum binding distances predicted by this procedure are illustrated in Figure 7 over a range of $\epsilon = 1 \rightarrow 40$. Since a dielectric constant of unity is too low for a protein our analysis suggests that the distance from the CPD to the FAD is 5.5−8 Å, representing a more realistic range of dielectric constants, $\epsilon = 2.6-10$, though the effective dielectric constant could be higher than this (*41*). The minimum distance is set by our transient absorption experiment, which implies that the substrate and cofactor are not in vdW contact.

DISCUSSION

Charge-Transfer Character of the Excited-State FAD in Photolyase. Oxidized photolyase's transient absorption spectrum provides insight into the electronic interactions between FAD and the protein matrix. The broad-band excited-state absorption in photolyase's spectrum is characteristic of a charge-transfer complex. This does not represent a charge-transfer complex with DNA, since it exists in the absence of substrate. Transient absorption spectra of fully reduced photolyase obtained by Okamura et al. (*42*) show the same broad-band excited-state absorption we observed in the oxidized species; however, the authors ascribed it to a singlet transition rather than a charge-transfer complex. Tryptophans 271, 277, 338, 382, and 384, as well as phenylalanine 366, are all aromatic amino acid residues in the immediate vicinity of FAD and, therefore, present themselves as candidates for charge-transfer coupling.

Previous work done in this lab (*19*) and others (*25*, *27*, *43*) suggests another possibility: the charge-transfer state may exist between isoalloxazine and adenine in FAD. Figure 4b reveals FAD's transient absorption spectrum to be intermediate between that of FMN, which is FAD without the adenosine moiety (Figure 4a), and photolyase (Figure 4c). Perhaps the unique proximal orientation of the adenine with respect to the isoalloxazine in photolyase acts to stabilize this charge-transfer state (the approximate structure of FAD in photolyase is shown in Figure 5, panels a and b). Further evidence for this theory is provided by the crystal structure of photolyase, which reveals the adenine to be adjacent to tryptophan 277. This suggests a possible pathway for electron transfer from the reduced isoalloxazine, to adenine, to tryptophan 277. Work is currently underway to explore this possibility.

Relevance of $\vec{F}_{CPD}$ for Dimer Repair by DNA Photolyase. The electric field produced by the CPD is an inevitable consequence of the large permanent ground-state dipole moment of pyrimidine and the coplanar configuration of the pyrimidine dimer. The field is large, about 3×10^8 V/m for a dimer at about 12 Å from the cofactor ($\epsilon = 1$), and will exist irrespective of the oxidation state of the flavin cofactor.

This distance is consistent with docking of substrate but inconsistent with the electronic coupling necessary to produce the observed (minimum) electron-transfer rate of less than $(100\ \text{ps})^{-1}$ (*44*, *45*). Antony et al. have approached the issue of substrate docking from the necessity of providing sufficiently large electronic coupling to produce ultrafast electron transfer (*46*). In their study, a coupling of $\sim 6\ \text{cm}^{-1}$ was required, which in turn places the CPD within about 3−5 Å of the flavin cofactor. For this structure, the dimer electric field would be enhanced by a factor of ∼100, adjusted for the permittivity of the protein. Hahn et al. predict that the *cis-syn* uridine-thymidine dimer will approach to within 9 Å of vdW contact based on semiempirical calculations (*33*). To date, however, no computational study has determined decisively what the cofactor−substrate distance is; the best experimental data from alanine substitution studies suggests that the dimer is deeply buried in the cavity near the flavin (*17*). This issue will likely be settled by an X-ray crystallographic structure of the enzyme−substrate complex; in any case the presence of a substantial electric field due to the dimer is strongly suggested by our model calculations.

The consequences of a strong substrate electric field may go far beyond a slight alteration in the protein's absorption spectrum. To understand how this field might affect electron transfer in photolyase it is useful to consider classical Marcus theory, where the electron-transfer rate, k_{et} is given as (*47*)

$$k_{et} \propto |V_{et}|^2 \frac{1}{\sqrt{4\pi\lambda kT}} e^{-(\Delta G^\circ + \lambda)^2/4\lambda kT} \qquad (4)$$

where V_{et} is the electronic coupling between donor (^{1}FADH$^-$) and acceptor (CPD), λ is the reorganization energy, ΔG° is the driving force of the reaction, and the exponential term represents the Franck−Condon overlap between the initial and final states. The distance dependence in k_{et} resides primarily in V_{et}, which depends exponentially on the overlap of the donor and acceptor orbitals. In the case of photolyase, if the donor−acceptor distance is large, 10−15 Å then electron transfer will be slow for direct electron transfer from cofactor to substrate (i.e., through-space electron transfer). This is significant because both low-temperature transient absorption studies (*45*) and low-temperature fluorescence quenching of the enzyme−substrate complex (*48*) suggest that electron transfer occurs in a temperature-independent (activationless) manner, $\Delta G^\circ \approx -\lambda$. This in turn suggests that a superexchange mechanism may be at work in photolyase (*46*, *49*). If this is true then there must be a virtual intermediate that is close in energy to the donor, quite possibly the adenine ring. The Franck−Condon factor also modulates k_{et} through the driving force ΔG° which is the energy difference between minima of the donor−acceptor nuclear potential wells.

Both the electronic and nuclear terms are susceptible to modulation by an electric field (*50*). The electric field can change the value of the argument in the exponent of the Franck−Condon factor if this field modulates the energy of a dipolar donor−acceptor complex (DA): $\Delta G^\circ + \lambda - \Delta\vec{\mu}_{et}\cdot\vec{F}_{CPD}$ where $\Delta\vec{\mu}_{et}$ is the difference dipole moment between the product D^+A^- and the reactant DA* for the field $\vec{F}_{CPD}$. To understand the sensitivity of k_{et} to this interaction energy, it is necessary to have values for the driving force and reorganization energy. This idea has been utilized for understanding the electron-transfer kinetics of the bacterial photosynthetic reaction center (*51*−*54*). Its relevance for photolyase depends on the orientation of $\Delta\vec{\mu}_{et}$ and $\vec{F}_{CPD}$.

Though an electric field effect on electron transfer in photolyase bears some resemblance to the reaction center problem, an important difference is that ions (i.e., FADH$^-$) do not have formal dipole moments. However, the difference dipole moment $\Delta\vec{\mu}_{et} = 2q\vec{r}_{et}$ where q is the charge of an electron and r_{et} is the electron-transfer distance (i.e., distance between the FADH$^-$ donor and the CPD acceptor) is defined and relevant (*55*). Using $r_{et} = 8$ Å ($|\Delta\vec{\mu}_{et}| = 78$ D) and a field strength of 2.7×10^8 V/m, we obtain a donor−acceptor interaction energy E_{DA} of about $\pm 3500\ \text{cm}^{-1}$ if the field and dipole are optimally aligned. From our calculations, we predict that the dimer field will be roughly in the same direction as $\Delta\vec{\mu}_{et}$, leading to a decrease in the exponent of eq 4.

Since electron transfer in the enzyme−substrate complex appears to be activationless, then $\Delta G^\circ + \lambda - \Delta\vec{\mu}_{et}\cdot\vec{F}_{CPD}$ is close to zero *only if the dipolar substrate has a particular orientation to the FAD cofactor*. Thus, it may be that the dimer electric field enhances the rate of electron transfer by tweaking the driving force to optimize the Franck−Condon factor of the Marcus expression if electron-transfer proceeds from ^{1}FADH$^-$ to the dimer in the direction of $\vec{F}_{CPD}$.

Interestingly, this type of argument can cut both ways when reverse electron transfer is considered, especially if the repaired thymidine bases continue to occupy the substrate cavity. Back electron transfer appears to be complete within about 2 ns (*42*, *45*, *56*, *57*) so that it is possible that the thymidine bases are relatively stationary over this time period. If the CPD field improves the electron-transfer rate to the dimer, then it is likely to act oppositely for the back electron-transfer step. Photodetachment spectroscopy on pyrimidine dimer anions suggests that a dipole moment of greater than 4 D is sufficient to create a "dipole trapped" electron (*38*, *39*, *58*). This complication suggests that it might be necessary to negate the effect of the CPD dipolar field to ensure reasonable electron-transfer rates in both the forward and reverse directions.

One possibility for ameliorating the electric field perturbation on the driving force is to have the field be perpendicular to $\Delta\vec{\mu}_{et}$. An examination of the crystal structure suggests that electron transfer from the isoalloxazine moiety to the adenine ring would involve charge transfer that is nearly orthogonal to the dimer electric field. Once on the adenine the electron is nearly in vdW contact with Trp 277 and much closer to the CPD. Either of these pathways are likely to have very large electronic couplings because of much larger orbital overlap relative to the CPD-FAD system.

Substrate Fields and Flavoprotein Electron Transfer. It has long been accepted that the electric field of the protein-binding site will be important in various aspects of catalysis (see refs *59*−*61* and references therein); however, little emphasis seems to be given to the electric field of the *substrate* in modulating the electron-transfer rate or mechanism (*62*). This is despite the fact the semiempirical and quantum mechanical calculations must implicitly take this field into account. The flavoprotein literature is replete with examples of spectral perturbations as the result of substrate binding. In many such instances, this is the result of charge-

transfer complexation between cofactor and substrate [two prominent examples are old yellow enzyme (*63*, *64*) and flavodoxin (*65*)] or binding of charged substrates.

In the present study, it is the substrate electric field, not charge transfer, which leads to the spectral perturbation. The dipolar electric field of the CPD is an intrinsic property of this substrate. Given the simplicity of our model and all the underlying approximations (i.e., dipole approximation for the field, approximate binding geometries, dielectric continuum model, etc.) we believe that the analysis provides convincing evidence for a substrate electric field that can alter the electron-transfer rate (and perhaps mechanism) in photolyase. However, photolyase may bind substrate in such a manner as to minimize the effect of the dipolar field to maintain an optimal electron-transfer (DNA repair) rate. It is tempting to consider that the dipolar substrates of other redox proteins must also engender large electric fields which may affect the driving force of the electron-transfer process. This may be true even when the protein does not require light for function and may be a general feature of flavoprotein mechanism not previously recognized.

ACKNOWLEDGMENT

A.W.M. gratefully acknowledges support from the PRF (ACS-35353-G4). We would like to thank Dr. Jianming Dai for his assistance with some of the transient absorption work. Professor Aziz Sancar (University of North Carolina, Chapel Hill) provided us with the pMS969 plasmid. Professor Walter Struve (Iowa State University) gave us advice on how to construct the rotating sample cell. Professor Olaf Wiest (University of Notre Dame) gave us help in obtaining his calculated photolyase structures. We also wish to thank Professor Alexei Stuchebrukhov (University of California, Davis) for interesting discussions on the electron-transfer mechanism in photolyase.

APPENDIX 1

Difference Dipole Moments of FAD, $\Delta\vec{\mu}_n^{FAD}$, in Photolyase from Stark Spectroscopy. From eq 1 it is necessary to know the magnitude of FAD's difference dipole moments and their orientation with respect to the dimer electric field, $\vec{F}_{CPD}$. Recently, we have published values for $\Delta\vec{\mu}_n^{FAD}$ for both $n = 1$, 2 transitions measured in relatively nonpolar solvents (*21*). The $S_0 \rightarrow S_1$ transition (band I) has a magnitude of $\Delta\vec{\mu}_1^{FAD} = 2.5 \pm 0.1$ *D*·*f* and makes an angle of 59° (±3) relative to the transition dipole moment, $\vec{m}_I$. This transition dipole moment lies in the plane of the isoalloxazine about 15° clockwise from the long axis of the molecule (*66*) and is roughly parallel to the ground-state dipole moment, $\vec{\mu}_0^{FAD}$ (*67*) (see Scheme 2 to obtain the sense of rotation relative to the pyrimidine end of the isoalloxazine). The 380 nm band (band II) has a much larger change in dipole moment for $S_0 \rightarrow S_2$ $\Delta\vec{\mu}_2^{FAD} = 7.5 \pm 0.1$ *D*·*f* with an angle of 24° (±6) relative to $\vec{m}_{II}$. This transition dipole moment is again in the isoalloxazine plane but rotated about 5° counterclockwise from the long axis of the molecule (*66*). The angle between $\vec{m}_{II}$ and $\vec{\mu}_0^{FAD}$ is roughly 20°. Stark measurements made on oxidized photolyase without substrate in a low temperature glycerol/buffer glass give roughly the same angle between transition dipole moment and difference dipole moment (*21*).

The difference dipole moments are not determined absolutely but must be multiplied by the local field factor *f* which is always greater than unity. *f* corrects for the local dielectric constant ϵ, but the form of *f* depends on the shape of the solvent cavity as well as on the dielectric constant of the solvent. We have used $f = 1.6$, calculated to account for the ellipsoidal shape of the FAD molecule in the relatively nonpolar solvent 2-methyltetrahydrofuran ($\epsilon = 7.6$) (*21*). This is a drastic simplification because the true correction factor will have to reflect the dielectric anisotropy of the protein binding site. However, in the *ratio* of the two difference dipole moments *f* will cancel. From eq 1, the ratio of the observed shifts will retain the essential element of the electrochromism model without the burden of defining an explicit correction factor.

Flavin's ground-state dipole moment ($\vec{\mu}_0^{FAD}$) was calculated for each of the models (flipped, B-DNA, and dinucleotide) by assigning partial charges supplied by Hall et al. (*67*) for atoms on the isoalloxazine ring. No account was made for the ribityl chain or adenine, which do not absorb light in the spectral region where the shift is observed. Dipole moments calculated in this manner vary slightly due to twisting of the modeled flavins out of the planar conformation, but all had magnitudes of 7.3 ± 0.1 D, and were within 2° of planarity with the flavin ring.

FAD's difference dipole moments ($\Delta\vec{\mu}_n^{FAD}$) in the coordinate system of the modeled active site were assigned directions by rotating the vectors about an axis normal to flavin's plane. This was accomplished by transforming a unit vector in the direction of $\vec{\mu}_0^{FAD}$ into a coordinate system where the flavin lay in the $x-y$ plane, rotating it about the *z* axis to the angle provided by our Stark measurements, then transforming the coordinates of the rotated vector back into the molecular frame: $\Delta\hat{\mu}_n^{FAD} = T_{nm}^{T} R_{ijk} T_{nm} \hat{\mu}_0^{FAD}$, where $\hat{\mu}_n^{FAD}$ is a unit vector in the direction of $\Delta\vec{\mu}_n^{FAD}$, $\hat{\mu}_n^{FAD}$ is a unit vector which points along $\vec{\mu}_0^{FAD}$, T_{nm} are matrix elements formed by dot product of unit vectors in the *n*th dimension of the molecular coordinate system with unit vectors in the *m*th dimension of a coordinate system in which the *z* axis is normal to the flavin plane. This *z* axis was assigned by taking the cross product of two vectors which point from C8 on the xylene ring of isoalloxazine to C7 and C9, respectively. R_{ijk} is the following rotation matrix:

$$R_{ijk} = \begin{bmatrix} \cos(\theta) & \sin(\theta) & 0 \\ -\sin(\theta) & \cos(\theta) & 0 \\ 0 & 0 & 1 \end{bmatrix} \qquad \text{(A.1)}$$

where θ represents the angle between $\vec{\mu}_0^{FAD}$ and $\vec{\mu}_1^{FAD}$ or $\vec{\mu}_2^{FAD}$. This directional vector was multiplied by the corresponding magnitude to provide values for $\vec{\mu}_n^{FAD}$.

APPENDIX 2

"Best Fit" Model. For this model all that is needed are a dinucleotide thymidine dimer (T<>T) and the isoalloxazine. The T<>T dimer was constructed using the NMR solution state structure of a dodecamer duplex DNA containing a CPD (1TTD.PDB) (*4*). The CPD dipole moment was then calculated by assigning partial charges reported by Hahn et al. (*33*) to the thymidine dimer and summing the charges times their distance relative to the (1TTD.PDB) center of

coordinates. FAD's difference dipole moments were assigned magnitudes and angles pointing from the center of a two-dimensional coordinate system based in the plane of the isoalloxazine heterocycle with flavin's ground-state dipole defining the *X* axis. A vector equal in magnitude to the calculated value for $\vec{\mu}_{CPD}$ was pointed in a direction derived by multiplying a unit vector along the *X* axis by

$$R_{ij} = \begin{bmatrix} \cos(\gamma) & \sin(\gamma) \\ -\sin(\gamma) & \cos(\gamma) \end{bmatrix} \quad (3)$$

where γ is the angle between $\Delta\vec{\mu}_n^{FAD}$ and $\vec{F}_{CPD}$.

REFERENCES

1. Jorns, M. S., Wang, B., Jordan, S. P., and Chanderkar, L. P. (1990) *Biochemistry 29*, 552−561.
2. Sancar, A., and Sancar, G. B. (1988) *Annu. Rev. Biochem. 57*, 29−67.
3. Fisher, G. J., and Johns, H. E. (1976) in *Photochemistry and Photobiology of Nucleic Acids* (Wang, S. Y., Ed.) pp 226−294, Academic Press, New York.
4. McAteer, K., Jing, Y., Kao, J., Taylor, J. S., and Kennedy, M. A. (1998) *J. Mol. Biol. 282*, 1013−1032.
5. Hanawalt, P. C. (1994) *Science 266*, 1957−1958.
6. Donahue, B. A., Yin, S., Taylor, J.-S., Reines, D., and Hanawalt, P. C. (1994) *Proc. Natl. Acad. Sci. U.S.A. 91*, 8502−8506.
7. Sancar, A. (1994) *Biochemistry 33*, 2−9.
8. Kato, R., Hasegawa, K., Hidaka, Y., Kuramitsu, S., and Hoshino, T. (1997) *J. Bacteriol. 179*, 6499−6503.
9. Malhotra, K., Kim, S. T., Walsh, C., and Sancar, A. (1992) *J. Biol. Chem. 267*, 15406−15411.
10. Jorns, M. S., Sancar, G. B., and Sancar, A. (1985) *Biochemistry 24*, 1856−1861.
11. Heelis, P. F., Okamura, T., and Sancar, A. (1990) *Biochemistry 29*, 5694−5698.
12. Jorns, M. S., Wang, B., and Jordan, S. (1987) *Biochemistry 26*, 6810−6816.
13. Sancar, G. B., Jorns, M. S., Payne, G., Fluke, D. J., Rupert, C. S., and Sancar, A. (1987) *J. Biol. Chem. 262*, 492−498.
14. Payne, G., and Sancar, A. (1990) *Biochemistry 29*, 7715−7727.
15. Park, H.-W., Kim, S.-T., Sancar, A., and Deisenhofer, J. (1995) *Science 268*, 1866−1872.
16. McCullough, A. K., Dodson, M. L., Scharer, O. D., and Lloyd, R. S. (1997) *J. Biol. Chem. 272*, 27210−27217.
17. Berg, B. J. V., and Sancar, G. B. (1998) *J. Biol. Chem. 273*, 20276−20284.
18. Slifkin, M. A. (1971) *Charge-Transfer Interactions of Biomolecules*, Academic Press, London.
19. Stanley, R. J., and MacFarlane, A., IV (2000) *J. Phys. Chem. A 104*, 6899−6906.
20. DeVoe, H., and Tinoco, I., Jr. (1962) *J. Mol. Biol. 4*, 500−517.
21. Stanley, R. J., and Siddiqui, M. S. (2001) *J. Phys. Chem. A* (In press).
22. Sancar, A., Smith, F. W., and Sancar, G. B. (1984) *J. Biol. Chem. 259*, 6028−6032.
23. Payne, G., Wills, M., Walsh, C., and Sancar, A. (1990) *Biochemistry 29*, 5706−5711.
24. Weber, G. (1950) *Biochem. J. 47*, 114−121.
25. Barrio, J. R., Tolman, G. L., Leonard, N. J., Spencer, R. D., and Weber, G. (1973) *Proc. Natl. Acad. Sci. U.S.A. 70*, 941−943.
26. Bastiaens, P. I. H., Van Hoek, A., Benen, J. A. E., Brochon, J. C., and Visser, A. J. W. G. (1992) *Biophys. J. 63*, 839−853.
27. Karen, A., Sawada, M. T., Tanaka, F., and Mataga, N. (1987) *Photochem. Photobiol. 45*, 49−53.
28. Mataga, N., Chosrowjan, H., and Shibata, Y. (1998) *J. Phys. Chem. B 102*, 7081−7084.
29. MacInnis, J. M., and Kasha, M. (1988) *Chem. Phys. Lett. 151*, 375−378.
30. Karen, A., Ikeda, N., Mataga, N., and Tanaka, F. (1983) *Photochem. Photobiol. 37*, 495−502.
31. Leenders, H. R. M., Vervoort, J., Van Hoek, A., and Visser, A. J. W. G. (1990) *Eur. Biophys. J. 18*, 43−55.
32. Yagi, K., Tanaka, F., Nakashima, N., and Yoshihara, K. (1983) *J. Biol. Chem. 258*, 3799−3802.
33. Hahn, J., Michel-Beyerle, M.-E., and Rösch, N. (1999) *J. Phys. Chem. B 103*, 2001−2007.
34. Sanders, D. B., and Wiest, O. (1998) *J. Am. Chem. Soc. 121*, 5127−5134.
35. Medvedev, D., and Stuchebrukhov, A. A. (2001) *J. Theor. Biol. 210*, 237−248.
36. Liptay, W. (1969) *Angew. Chem., Int. Ed. 8*, 177−188.
37. Duschene, J. (1973) *Physico-Chemical Properties of Nucleic Acids*, Academic Press, New York.
38. Durbeej, B., and Eriksson, L. A. (2000) *J. Am. Chem. Soc. 122*, 10126−10132.
39. Voityuk, A. A., and Rösch, N. (1997) *J. Phys. Chem. A 101*, 8335−8338.
40. McHale, J. L. (1999) *Molecular Spectroscopy*, Prentice Hall, Upper Saddle River.
41. Voityuk, A. A., Michel-Beyerle, M.-E., and Rösch, N. (1996) *J. Am. Chem. Soc. 118*, 9750−9758.
42. Okamura, T., Sancar, A., Heelis, P. F., Begley, T. P., Hirata, Y., and Mataga, N. (1991) *J. Am. Chem. Soc. 113*, 3143−3145.
43. McCormick, D. B. (1977) *Photochem. Photobiol. 26*, 169−182.
44. Kim, S. T., Heelis, P. F., Okamura, T., Hirata, Y., Mataga, N., and Sancar, A. (1991) *Biochemistry 30*, 11262−11270.
45. Langenbacher, T., Zhao, X., Bieser, G., Heelis, P. F., Sancar, A., and Michel-Beyerle, M. E. (1997) *J. Am. Chem. Soc. 119*, 10532−10536.
46. Antony, J., Medvedev, D. M., and Stuchebrukhov, A. A. (2000) *J. Am. Chem. Soc. 122*, 1057−1065.
47. Marcus, R. A., and Sutin, N. (1985) *Biochim. Biophys. Acta 811*, 265−322.
48. Rustandi, R. R., and Jorns, M. S. (1995) *Biochemistry 34*, 2284−2288.
49. Weber, S., Moebius, K., Richter, G., and Kay, C. W. M. (2001) *J. Am. Chem. Soc. 123*, 3790−3798.
50. Lockhart, D. J., Kirmaier, C., Holten, D., and Boxer, S. G. (1990) *J. Phys. Chem. 94*, 6987−6995.
51. Boxer, S. G. (1990) *Annu. Rev. Biophys. Biophys. Chem 19*, 267−299.
52. Ogrodnik, A., Langenbacher, T., Bieser, G., Siegl, J., Eberl, U., Volk, M., and Michel-Beyerle, M. E. (1992) *Chem. Phys. Lett. 198*, 653−658.
53. Eberl, U., Ogrodnik, A., and Michel-Beyerle, M. E. (1990) *Z. Naturforschung, Teil A 45a*, 763−770.
54. Boxer, S. G. (1996) *Adv. Photosynth. 3*, 177−189.
55. Shin, Y.-G. K., Brunschwig, B. S., Creutz, C., and Sutin, N. (1995) *J. Am. Chem. Soc. 117*, 8668−8669.
56. Kim, S. T., Heelis, P. F., and Sancar, A. (1992) *Biochemistry 31*, 11244−11248.
57. Kim, S.-T., Volk, M., Rousseau, G., Heelis, P. F., Sancar, A., and Michel-Beyerle, M.-E. (1994) *J. Am. Chem. Soc. 116*, 3115−3116.
58. Schiedt, J., Weinkauf, R., Neumark, D. M., and Schlag, E. W. (1998) *Chem. Phys. 239*, 511−524.
59. Lockhart, D. J., and Kim, P. S. (1992) *Science 257*, 947−951.
60. Lockhart, D. J., and Kim, P. S. (1993) *Science 260*, 198−202.
61. Dinakarpandian, D., Shenoy, B. C., Hilvert, D., McRee, D. E., McTigue, M., and Carey, P. R. (1999) *Biochemistry 38*, 6659−6667.
62. Kaposi, A. D., Wright, W. W., Fidy, J., Stavrov, S. S., Vanderkooi, J. M., and Rasnik, I. (2001) *Biochemistry 40*, 3483−3491.

63. Brown, B. J., Deng, Z., Karplus, P. A., and Massey, V. (1998) *J. Biol. Chem. 273*, 32753−32762.
64. Massey, V., and Schopfer, L. M. (1986) *J. Biol. Chem. 261*, 1215−1222.
65. Swenson, R. P., and Krey, G. D. (1994) *Biochemistry 33*, 8505−8514.
66. Eaton, W. A., Hofrichter, J., Makinen, M. W., Andersen, R. D., and Ludwig, M. L. (1975) *Biochemistry 14*, 2146−2151.
67. Hall, L. N., Orchard, B. J., and Tripathy, S. K. (1987) *Int. J. Quant. Chem. 31*, 217−242.

BI0114224